

Development of IR Single Mode Optical Fibers for DARWIN-nulling Interferometry

Shahina M. C. Abdulla¹, Lun-Kai Cheng¹, Boudewijn v.d. Bosch¹, Niels Dijkhuizen¹, Remco Nieuwland¹, Wim Gieleesen¹, Jaques Lucas², Catherine Boussard-Plédel², Clément Conseil², Bruno Bureau² and João Pereira Do Carmo³

¹TNO, Stieltjesweg 1, 2628 CK, Delft, The Netherlands

²University of Rennes, Glass and Ceramic Laboratory, Campus of Beaulieu, 35042 Rennes, France

³European Space Agency, P.O. Box 299, 2200 AG, Noordwijk ZH, The Netherlands

Keywords: Single Mode Fibers, Nulling Interferometry, DARWIN, Chalcogenide Glass, Infrared, Far Field Intensity, Cross Core Scan, TeAsSe Fibers, TeGeGaI, Higher Order Mode Suppression.

Abstract: The DARWIN mission aims to detect weak infra-red emission lines from distant orbiting earth-like planets using nulling interferometry. This requires filtering of wavefront errors using single mode waveguides operating at a wavelength range of 6.5-20 μm . This article describes the optical design of the fibers, the manufacturing protocol, the packaging for operating at cryogenic environment and various optical characterisations performed. The latter includes investigation on the effect of gold and silver absorption coatings, anti-reflection coating, fiber length on higher order mode suppression and attenuation of the fibers.

1 INTRODUCTION

The DARWIN mission by the European Space Agency (ESA) (Woolf, 1998) is aimed to locate and study earth like planets in other solar systems, in a search for extra-terrestrial life (Kaltenegger, 2005). DARWIN will consist of a nulling interferometer (Bracewell, 1978); (Angel, 1978); (Spronck, 2012), combining light from several telescopes that are phase shifted from each other. This nulling technique results in the light from a bright star being cancelled out, leaving only light from the planets around the star. Such a system, with capability for imaging and spectroscopy, operating in the thermal infrared spectral region, requires that wavefront errors be reduced to a very high degree, in order to achieve the required nulling quality (10^{-4} to 10^{-6}). Such a high wavefront quality can only be achieved with adequate wavefront filtering measures.

Modal filters like single mode fibers are the preferred solution since they can filter both low and high spatial frequencies (Bracewell, 1978); (Angel, 1978). Potential technologies for the development of single mode fibers either using Step Index Fibers (SIF's) or Index Guiding Photonic Crystal Fibers (IG-PCF's) have been studied (Cheng, 2005)

(Zhukova, 2012) (Spronck, 2012). This article describes the results on the development of Single Mode Waveguides (SMW's) based on SIF's, typically made of a solid material core and cladding having slightly different refractive indices (n). For a properly designed fiber, in the operational wavelength range, the fundamental mode is only guided by the core and the higher order modes (HOMs) will experience a strong attenuation. After a certain length of the fibre only the fundamental mode remains. The wavelength limit for single mode operation is mainly determined by the core diameter, the symmetry of the core cross-section and the difference in refractive index between core and cladding which needs to be controlled very accurately to achieve the required performance.

Table 1: Main requirements for the fibres to be used in DARWIN mission.

| Parameter | Requirement |
|------------------------------|-------------------------|
| Operational wavelength range | 6.5 to 20 μm |
| Nr. of wavelength sub-bands | ≤ 3 |
| Total transmission | $> 57\%$ |
| HOM suppression ratio | $< 10^{-4}$ |
| Operational temperature | 40 K |
| Maximum SMW dimension | 40 cm |
| Polarisation | ≤ 2.5 mrad |

Since in reality the cladding diameter is finite, HOMs will be guided by the cladding. Here additional absorption coatings will be required to suppress these cladding modes.

The main requirements for the fibres to be used in DARWIN mission are summarized in the Table 1.

2 FIBER DESIGN

The focus of this research programme was to develop manufacturing techniques for a reproducible production of single mode SIF's, aiming to result in wavefront filters covering the complete DARWIN wavelength range which can be directly used in interferometric test set-ups operating in vacuum and cryogenic environment. To this respect two major types of chalcogenide glass materials, potentially suitable for SIF manufacturing in the wavelength range of interest for DARWIN, were identified and investigated. The first one is TeAsSe (TAS) (Cheng, 2006); (Faber, 2006) glass for the short wavelength (SW) range (6.5 μm –12 μm). Several manufacturing techniques were explored resulting in the manufacturing of several SIF samples from this material and single mode behaviour was demonstrated by Far Field Intensity (FFI) distribution. The relation between the composition and the refractive index of this type of fibers were investigated. A proper selection of the composition of the TAS glass will result in the desired refractive index for the core and the cladding. The default design parameters are:

| | |
|--------------------------------|---|
| - n -core: | 2.9185 |
| - Core radius: | 17.5 μm |
| - n -cladding: | 2.9157 |
| - Cladding thickness: | 250 μm |
| - Numerical Aperture (NA): | 0.13 |
| - Cut-off wavelength: | 5.7 μm |
| - Absorption coating: | Gallium (Ga) |
| - AR coating: | BaF ₂ /ZnSe/BaF ₂ |

The second type of chalcogenide glass material is Te-based glass for the long wavelength (LW) range (12 μm – 20 μm) for which development was less mature. It was demonstrated that Te-glasses are potentially suitable for fiber manufacturing purposes but still critical with respect to processing parameters and risk of crystallization (Cheng, 2006). Some Te-glass based materials are investigated. The TeGeGaI (TGGI) glass is selected for the LW fiber design. A typical transmission spectrum of a TGGI glass of about 2mm is shown in Figure 1.

For the TGGI based LW fiber only a provisional default fiber design is defined:

| | |
|-----------------------|--------------------|
| - n -core: | 3.350 |
| - Core radius: | 15 μm |
| - n -cladding: | 3.338 |
| - Cladding thickness: | 250 μm |
| - NA : | 0.29 |
| - Cut-off wavelength: | 11.3 μm |
| - Absorption coating: | Gallium |
| - AR coating: | Not defined. |

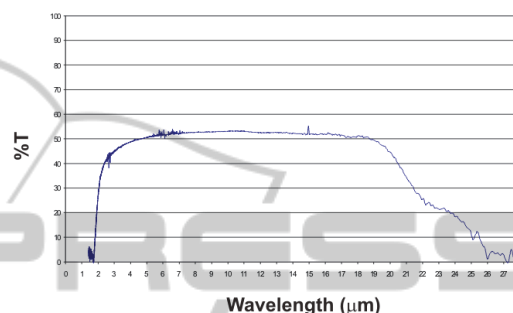


Figure 1: Transmission spectrum of TGGI shows a transmission window up to about 19 μm .

2.1 Development of Absorption Coating

To ensure a sufficient nulling depth, the amount of optical power in the higher order modes at the output of the single mode fiber must be reduced. The HOM suppression performance depends on the thickness of the cladding and the imaginary part of the refractive index (k) of the absorption coating material applied. A material with a higher k is expected to have a higher absorption than a material with a lower k . Though Ga was successfully demonstrated to be a suitable coating, it was difficult to apply a homogeneous layer. Further handling was critical due to the low melting point of Ga. Even at room temperature Ga becomes soft and mechanically unstable. To find a suitable alternative material as absorption coating, with better manufacturability, ease in handling and stability (and if possible better absorption), Finite Element Modelling of the SW TAS fiber was performed by Optoelectronics Research Centre of University of Southampton using a commercial software package called COMSOL Multiphysics™. The TAS SW fiber with different coating materials including Cr ($k_{Cr} \approx 15$ at 10.6 μm) and Ga ($k_{Ga} \approx 30$ at 10.6 μm) are modelled and the effect on attenuation and HOM are calculated (Cheng, 2009).

Modelling results confirm the expectation that $k_{Ga} > k_{Cr}$ requires a shorter fiber length (L) to

achieve a HOM suppression of 10^6 . The modelling also yielded that the attenuation, the fiber NA and cut-off wavelength are unaffected by the type of coating applied. Hence it was concluded that the absorption coatings can be developed separately from fiber configuration. A survey of suitable alternative coating materials is conducted with the following criteria:

- a k close to or higher than that of Ga (further reduction of the required fiber length).
- a thermal expansion, close to TAS (to survive temperature range down to 40 K).
- clean and easy deposition method (preferably vacuum deposition)

Finally, gold and silver were selected as absorption coatings for the final evaluation.

2.2 Development of AR Coating

For IR single mode fibers, having a $n > 2$, the loss by Fresnel reflection will be more than 11% per fiber interface. Suitable AR coatings therefore are required to maintain sufficient transmission. Using thin-film modelling, TNO investigated the performance of various AR coating configurations.

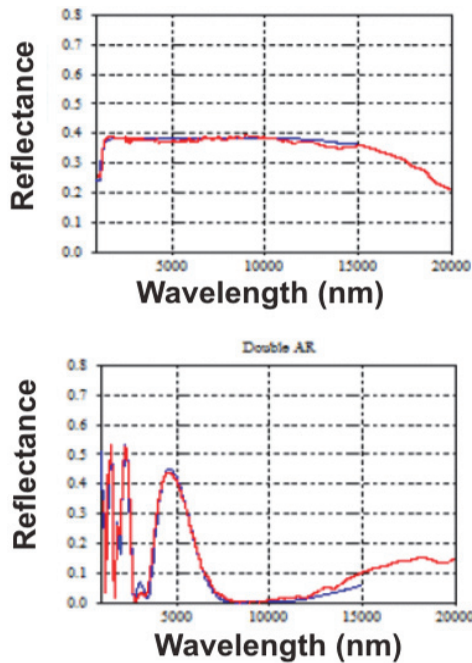


Figure 2: Demonstration of the effect of the designed AR coating. Reflection of a bulk TAS sample (top). Reflection of the same TAS sample with AR coating on both sides (bottom).

A three-layer coating configuration of

$BaF_2/ZnSe/BaF_2$ is considered to be a suitable candidate for the chalcogenide TAS glass. This AR coating design is further fine-tuned on TAS bulk samples. Transmission and reflection of the final configuration are measured. A TAS sample without coating is also tested for reference. The results are presented in Figure 2, showing a significant reduction of the reflection of double AR coated TAS compared to the uncoated TAS in the spectral region $6.5 - 12 \mu m$.

3 SW TAS FABRICATION PROTOCOL

Manufacturing protocols for purification and preparation of TAS glass and the fabrication of the fiber are established. The right composition, purification and temperature control are of vital importance for quality of the parts and for the fiber performance and hence have direct impact to the performance of the fiber produced.

The control of the composition and hence the refractive index of the TAS glasses is found to be very critical. Relaxing the refractive index tolerance is highly desirable to improve the manufacturing yield. This results in a larger difference between the refractive index of the core and the cladding. To ensure single mode operation starting from $6.5 \mu m$, the diameter of the core has also to be adapted. For the final design, the core radius is reduced from $17.5 \mu m$ to $11 \mu m$. The TAS SW fiber manufacturing protocol using a special developed 2-steps rod-in-tube technique is shown in Figure 3.

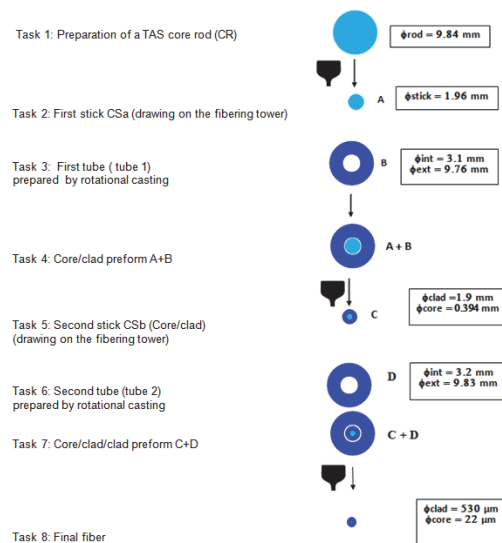


Figure 3: Manufacturing protocol of the TAS SW fiber.

4 TAS FIBER MANUFACTURING

For the manufacturing of TAS cladding tubes, rotational casting is applied (Figure 4). The dedicated set-up, manufacturing processes and parameters have been calibrated and optimized as the quality of the tube is highly influenced by the proper levelling of the set-up, temperature during rotational casting and rotation speed (Houizot, 2009). TAS tubes are manufactured with internal diameter ranging from 2.8 mm – 3.2 mm.

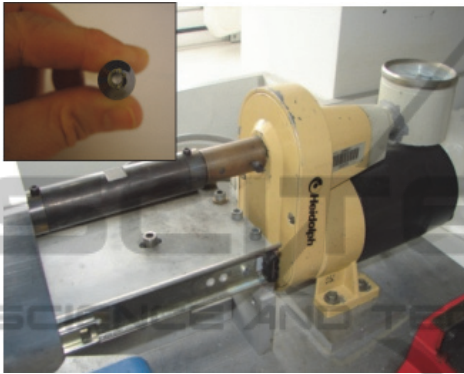


Figure 4: Rotational casting machine and resulting TAS tube (inset).

Based on TAS cladding glass composition and known refractive index results, the TAS core glass composition is defined. Purified core rods (CR) having an external diameter of ~10 mm are manufactured. The CR is drawn to a \varnothing 2 mm core stick having a length of about 60 cm (for core-clad preform drawing) and several meters of \varnothing 400 μ m mono-index fiber (used for fiber quality verification).

5 CHARACTERISATION

Prior to the characterization, each SMW is visually inspected for cracks or holes on the SMW surface along its length. Both facets of the SMW are carefully cleaved. The cleave which is not part of the SMW, is further visually inspected under a microscope to check the surface quality of the cross-section as well as the angle of the cleave. The optical measurements are performed using the set-up shown in Figure 5. The source is a CO₂ laser at 10.6 μ m having a built-in Helium-Neon laser which is used for alignment. A razor blade is used as a beam splitter. The output power of the CO₂ laser fluctuates about 20% (peak to peak) at 6% output power. It is undesired to use higher power since it can damage

the fibre. Hence during the measurements, a reference detector (with power P_{ref}) is used in the used range which is 3% - 7% of the output power.

- 1: Razor blade beamsplitter
- 2: Offaxis parabola
- 3: Pinhole on x-y-z-stage
- 4: x-y-z-stage with SMW
- A: Detector A
- B: Reference Detector B

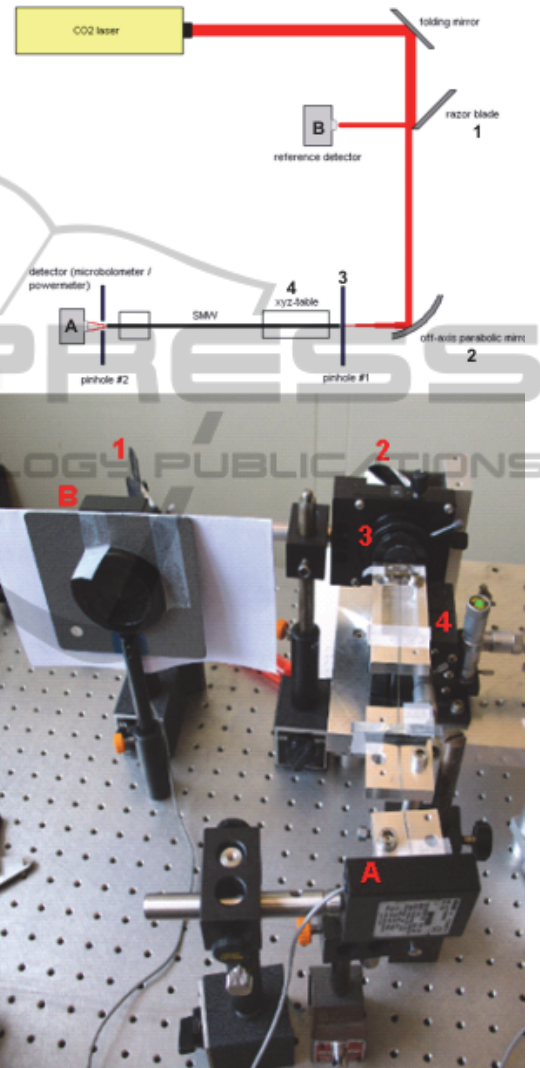


Figure 5: Pulsed CO₂ laser set-up for fiber attenuation and FFI characterization at 10.6 μ m. They are numbered as 1- Razor blade beamsplitter, 2- Off axis parabola, 3- Pinhole on x,y,z stage, 4- xyz stage with SMW, A is detector A and B is the reference detector B.

Several measurements are performed using this set-up and detailed explanation of the results are presented in the following sections.

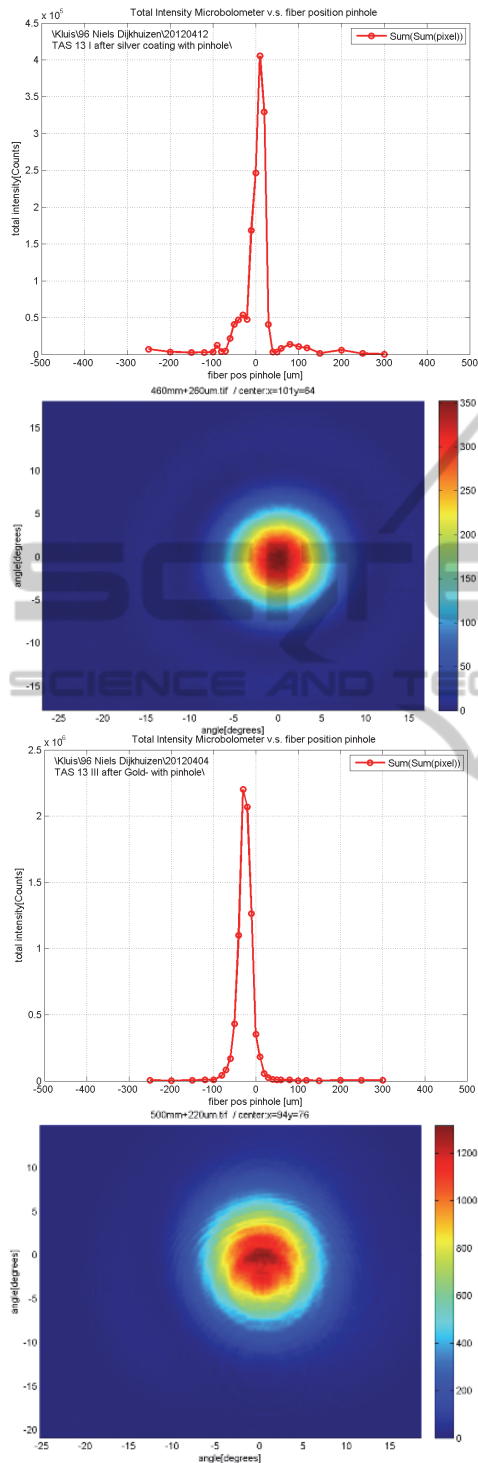


Figure 6: Cross-core and FFI performance of silver (top two pictures, $L=480\text{mm}$) and gold (bottom two pictures, $L=495\text{mm}$) coated TAS fibers. The output pinhole diameter is $100\ \mu\text{m}$ and the P_{ref} is 130mW in both cases.

5.1 Gold and Silver Absorption Coatings on TAS

Due to its improved quality in manufacturability, reproducibility, ease in handling and stability compared to gallium, gold and silver are selected as alternative absorption coatings for TAS fibers in order to suppress the HOMs. Hence TAS fibers are coated with gold and silver and are further characterised with cross-core scan and FFI distribution. The results of two samples (one silver coated and the other gold coated) are shown in Figure 6. All coated TAS samples show single mode behaviour with an averaged NA of 0.22 . From performance point of view both gold and silver demonstrate to be good alternatives but gold is preferred for its durability (no oxidation) and acceptance in space applications.

5.2 Effect of Fibre Length on Higher Order Mode Suppression

Also the impact of reduction in fibre length to the level of HOM suppression has been investigated. For this, a silver coated and a gold coated sample were selected and their lengths are reduced in steps. Then cross-core scan and FFI distribution were measured at each length. The silver coated sample is reduced in 2 steps to a final length of 16.5cm (still showing good performance with output pinhole) and the gold coated sample is reduced in 3 steps to a final length of 24cm . The results for the silver coated TAS sample at each cut-back length are shown in Figure.

It was observed that, without pinhole, both silver and gold coated fibers showed a decrease in HOM suppression, with a shorter fiber length. By using a $100\ \mu\text{m}$ output pinhole, the change in HOM suppression due to length reduction was not observed. Apparently the output pinhole had more effect than fiber length. The silver coated TAS samples showed a deviation in NA for different cutback lengths. This observation also drove to finally select gold as preferred absorption coating for further experiments. A consistency in NA was observed for the gold coated TAS sample ($NA = 0.20$) for all cutback lengths, both “with” and “without” pinhole.

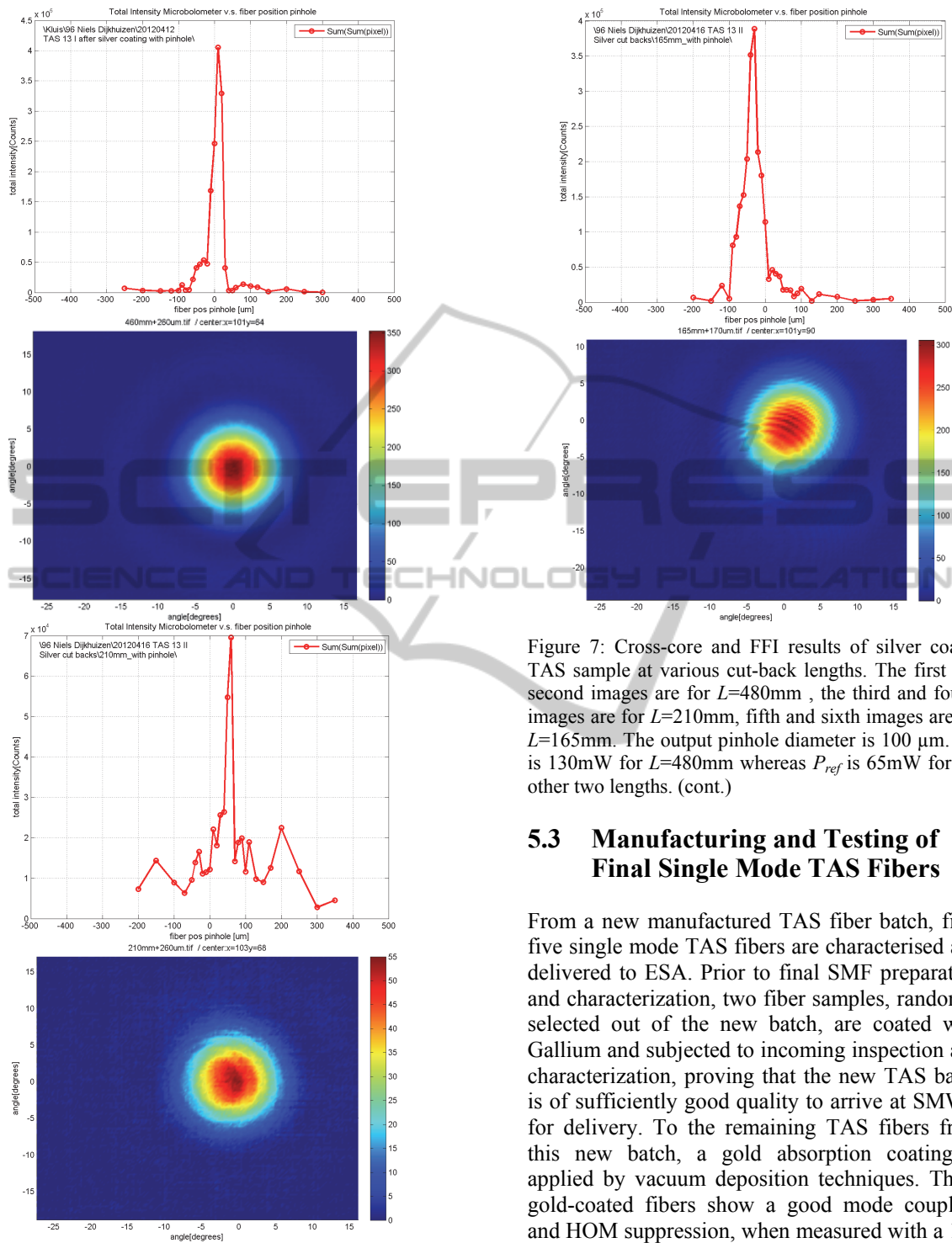


Figure 7: Cross-core and FFI results of silver coated TAS sample at various cut-back lengths. The first and second images are for $L=480\text{mm}$, the third and fourth images are for $L=210\text{mm}$, fifth and sixth images are for $L=165\text{mm}$. The output pinhole diameter is $100\ \mu\text{m}$. P_{ref} is 130mW for $L=480\text{mm}$ whereas P_{ref} is 65mW for the other two lengths.

Figure 7: Cross-core and FFI results of silver coated TAS sample at various cut-back lengths. The first and second images are for $L=480\text{mm}$, the third and fourth images are for $L=210\text{mm}$, fifth and sixth images are for $L=165\text{mm}$. The output pinhole diameter is $100\ \mu\text{m}$. P_{ref} is 130mW for $L=480\text{mm}$ whereas P_{ref} is 65mW for the other two lengths. (cont.)

5.3 Manufacturing and Testing of Final Single Mode TAS Fibers

From a new manufactured TAS fiber batch, final five single mode TAS fibers are characterised and delivered to ESA. Prior to final SMF preparation and characterization, two fiber samples, randomly selected out of the new batch, are coated with Gallium and subjected to incoming inspection and characterization, proving that the new TAS batch is of sufficiently good quality to arrive at SMW's for delivery. To the remaining TAS fibers from this new batch, a gold absorption coating is applied by vacuum deposition techniques. These gold-coated fibers show a good mode coupling and HOM suppression, when measured with a $100\ \mu\text{m}$ output pinhole as shown in Figure 8.

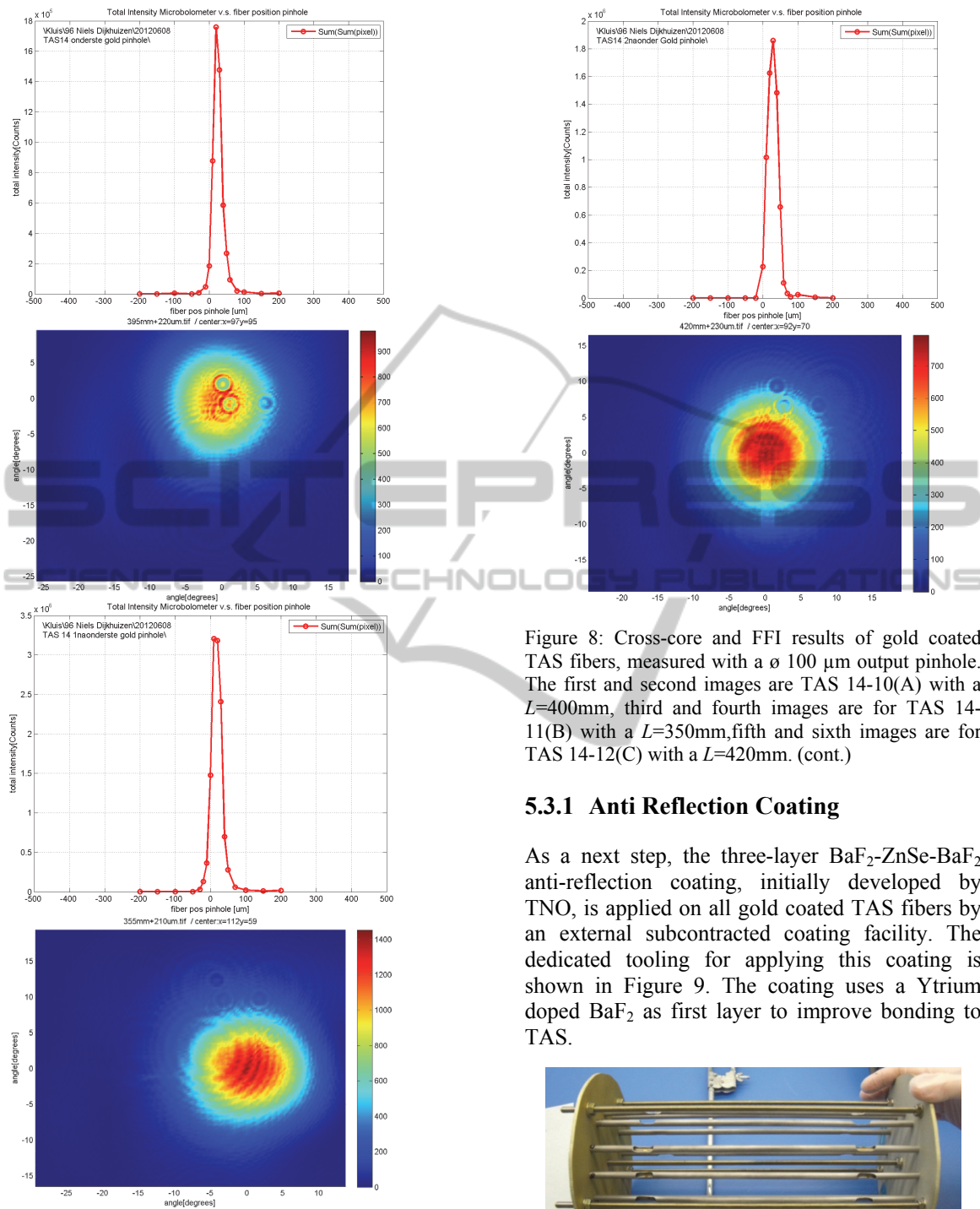


Figure 8: Cross-core and FFI results of gold coated TAS fibers, measured with a \varnothing 100 μ m output pinhole. The first and second images are TAS 14-10(A) with a $L=400$ mm, third and fourth images are for TAS 14-11(B) with a $L=350$ mm, fifth and sixth images are for TAS 14-12(C) with a $L=420$ mm.

Figure 8: Cross-core and FFI results of gold coated TAS fibers, measured with a \varnothing 100 μ m output pinhole. The first and second images are TAS 14-10(A) with a $L=400$ mm, third and fourth images are for TAS 14-11(B) with a $L=350$ mm, fifth and sixth images are for TAS 14-12(C) with a $L=420$ mm. (cont.)

5.3.1 Anti Reflection Coating

As a next step, the three-layer BaF_2 -ZnSe- BaF_2 anti-reflection coating, initially developed by TNO, is applied on all gold coated TAS fibers by an external subcontracted coating facility. The dedicated tooling for applying this coating is shown in Figure 9. The coating uses a Yttrium doped BaF_2 as first layer to improve bonding to TAS.

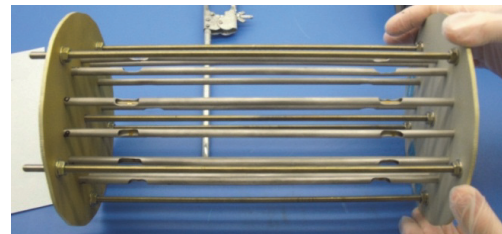


Figure 9: Tooling used for AR coating.

Jointly with the external coating facility, precautions were taken and arrangements were made to optimize the fabrication process for the

new special AR coating on both facets of the TAS fibers. Due to the limited available time, the fabrication process cannot be tested. For almost all coated TAS fibres, the AR coating delaminated from both fiber end facets and in some cases only the thin first layer of Yttrium doped BaF₂ remained on the fiber end. Figure 10 shows microscopic images of some of the fiber facets showing delaminated AR coating.

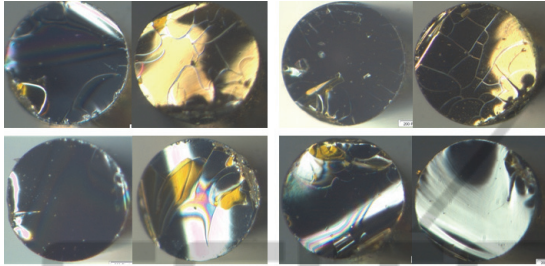


Figure 10: Some examples of delaminated AR coating on TAS end facets.

Cleaning of the fiber ends in an attempt to remove the delaminating AR coating was only in some cases successful. In most cases however the cleaning appeared to be less effective. Hence it was decided that cleaving of the TAS fiber end facets is the best solution to remove the faulty AR coatings. Thus the final single mode TAS fibers were delivered to ESA without an AR coating.

5.3.2 Cryo Testing



Figure 11: Photographs of cryogenic test set-up and Helium facility (SRON) for controlled 40K cycle tests.

Two gold coated TAS fibers were mounted in the special designed cryogenic copper SMW holder and were subjected to a controlled cryo-test (1 cycle for more than 2 hours at 40K), using a Helium cryostat facility of Netherlands Institute for Space research (SRON) as shown in Figure 11.

Following the cryo-cycle test, visual inspection did not show any significant change of the copper holders nor any failure/degradation of the TAS fibers after de-mounting from the holder. Microscopic inspections proved that the quality of the fiber end facets and gold coated surfaces did not degrade due to the 40K exposure. Also the FFI performance remained still good after cryo-tests.

5.3.3 Copper Mounting

For delivery to ESA, five gold coated TAS fibers, having no AR coating are selected and mounted in the special designed cryogenic copper SMW holders. The mounted fibers are delivered without SMA connector interface but with the fiber end facets protruding outside the holder for a few millimetres at both sides of the mount.

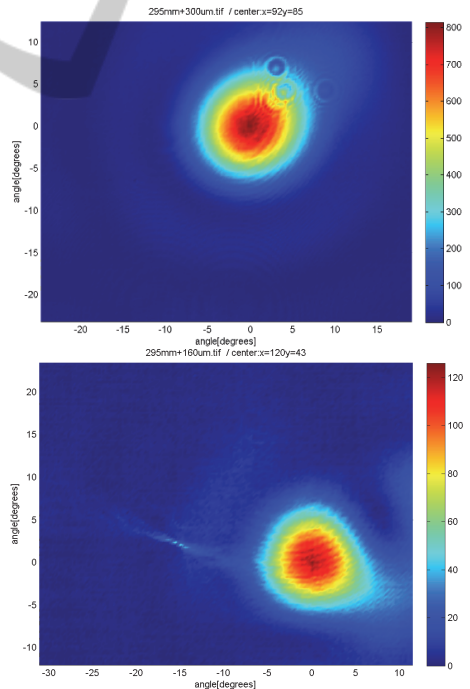


Figure 12: Cross-core and FFI characterization of the five packaged TAS fibers. First image is TAS 14-1 in (Cu holder 1), second image is TAS 14-2 in (Cu holder 2), third image is TAS 14-5 in (Cu holder 3), fourth image is TAS 14-6 in (Cu holder 5), and the fifth image is TAS 14-7 in (Cu holder 4). The output pinhole diameter is 100 μm and P_{ref} is 100mW.

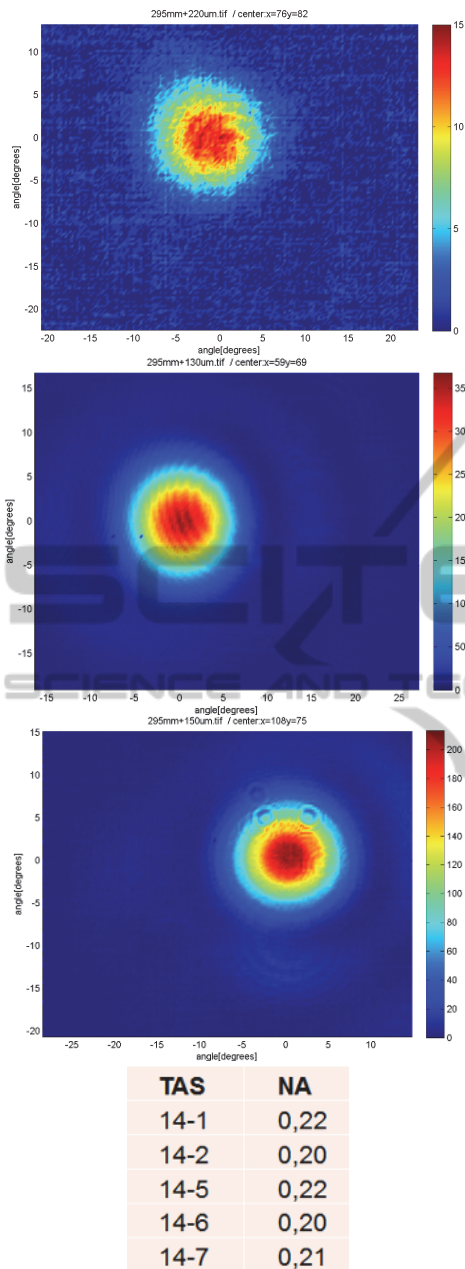


Figure 12: Cross-core and FFI characterization of the five packaged TAS fibers. First image is TAS 14-1 in (Cu holder 1), second image is TAS 14-2 in (Cu holder 2), third image is TAS 14-5 in (Cu holder 3), fourth image is TAS 14-6 in (Cu holder 5), and the fifth image is TAS 14-7 in (Cu holder 4). The output pinhole diameter is 100 μm and P_{ref} is 100mW. (cont.)

The length of these fibers range from 288 mm to 292 mm. After packaging, the cross-core scan and FFI distribution of each fiber was measured and the results of it are shown in Figure 12. All five fibers show a clear single mode behaviour.

With a 100 μm output pinhole they showed a strong circular FFI distribution. The NA of these fibers range from 0.20 to 0.22.

For safe transport, storage and handling (when not in use) of the fibers, which are mounted in the copper holder, the packages were provided with removable protection caps at both ends of the mount. This will protect the TAS fiber end facets protruding from the mount. Figure 3 shows these five fibers packaged inside five copper holders including protection caps in the final configuration delivered to ESA.

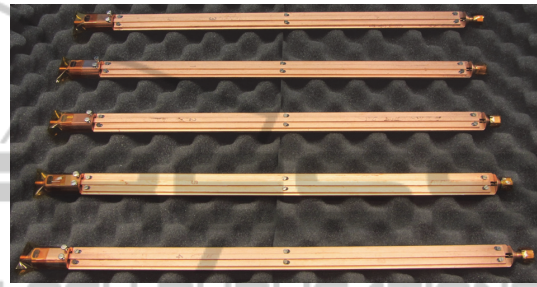


Figure 13: Five TAS fibers fully packaged as delivered to ESA.

6 CONCLUSIONS

A number of conclusions were drawn from the characterisations performed on single mode waveguides. Modelling of the impact of Ga coating on HOM suppression of a short wavelength TAS fiber shows that the NA and cut-off wavelength are not affected by the type of absorption coating applied. According to simulation, Ga with a higher k than Cr requires a shorter fiber length to achieve the desired HOM suppression. Further accurate measurement of refractive index is of vital importance for fiber design optimization. The quality and purity of the base materials determine largely the final SMF results and performance. Effectiveness of vacuum deposited silver and gold as absorption coating is comparable to that of the Gallium coating. However, gold coating is more stable and can be applied and handled more easily. Therefore the gold coating is selected for the final deliverable fibers. The suppression of cladding modes on an absorption coated fiber increases with its length. However, even for a length of about 500mm, the presence of cladding modes can still be observed in the FFI measurement. The application of an output pinhole of 100 μm diameter improves this suppression significantly. AR coating design is

optimized and the performance of this coating on bulk TAS sample is demonstrated successfully. Proper design of a copper fiber holder for cryogenic temperature application is investigated and realized. Cryogenic test with gold coated TAS fibers mounted in this holder has proven that the TAS fibers successfully survives cool down to 40 K without visible degradation or failure. Five short wavelength TAS single mode waveguides with gold absorption coating but without AR coating are integrated in the fiber holder and characterised by cross core scan and FFI.

ACKNOWLEDGEMENTS

This project was funded by the European space Agency under the contract No. 20914/07/NL/CP. The authors would like to thank the Optoelectronics Research Centre of University of Southampton for the modelling of the cladding mode suppression and Netherlands Institute for Space research (SRON) for providing their Cryogenic facility.

REFERENCES

- Woolf, N., and Angel, J., 1998 "Astronomical searches for earth-like planets and signs of life," *Astron.Astrophys.*36, pp. 507-537.
- Kaltenegger, L., Fridlund, M., 2005, "The Darwin mission: Search for extra-solar planets", *Advances in Space Research* 36, pp 1114-1122.
- Bracewell, R. N., 1978 "Detecting nonsolar planets by spinning infra-red interferometer", *Nature* 274, pp 780-781.
- Angel, J. R. P., Cheng, A. Y. S., and Woolf, N. J., 1978 "A space telescope for infra-red spectroscopy of earth like planets", *Nature* 322, pp 341-434.
- Cheng, L. K., Faber, A. J., Gielesen, W., Boussard-Plédel, C., Houizot, P., Lucas, J., and Pereira Do Carmo, J., 2005 "Test results of the infrared single-mode fiber for the DARWIN mission," *Proceedings of SPIE* 5905, 59051F.
- Cheng, L. K., Faber, A. J., Gielesen, W., Lucas, J., Boussard-Plédel, C., Houizot, P., and Pereira do Carmo, J., 2006 "Development of broadband infrared single-mode fibers for the DARWIN mission," *Proceedings of SPIE* 6268, 62682F.
- Faber, A. J., Cheng, L. K., Gielesen, W. L. M., Boussard-Plédel, C., Houizot, P., Danto, S., Lucas, J., and Pereira Do Carmo, J., 2006, "Single Mode Chalcogenide Glass Fiber as Wavefront Filter for the Darwin Planet Finding Mission," *Proceedings of '6th International. Conference. on Space Optics' ESTEC*, pp. 27-30.
- Cheng, L. K. et al., 2009, "Development of infrared single-mode fibers for 2 wavelength bands of the Darwin mission: Test results of prototypes", *Proceedings of SPIE* 7420.
- Houizot, P., Boussard-Plédel, C., Faber, A. J., Cheng, L. K., Bureau, B., Van Nijnatten, P. A., Gielesen, W. L. M., Pereira do Carmo, J., and Lucas, J., 2007, "Infrared single mode chalcogenide glass fiber for space," *Optics Express* 15 (19), pp 12529-12538.
- Zhukova, L., Korsakov, A., Chazov, A., Vrublevsky, D. and Zhukov, V., 2012, "Photonic crystalline IR fibers for the spectral range of 2–40 μm ", *Applied Optics* 51, pp. 2414-2418.
- Spronck, J. F. P., Fischer, D. A. and Kaplan, Z. A., 2012, "Use and limitations of single-and multi-mode optical fibers for exoplanet detection." *Optical Fibers/Book 3.*